Scaling of the volume-related effective power for ultrasonic tanks of different sizes

Andreas Hertz-Eichenrode, Reinhard Sobotta and Christoph Jung

Elma Schmidbauer GmbH, D-Singen

1. Introduction

Often there is a demand to scale up the ultrasonic design after successful cleaning tests in small devices to ultrasonic tanks of bigger volume for industrial cleaning equipment. Besides other factors (chemistry, temperature and dwell-time) the success of the cleaning test was ensured by the operation of the small device above the threshold of inertial cavitation. Then the design of the ultrasonics for the bigger tanks has to guarantee a crossing of the threshold there also.

There is a method /1/ for the measurement of the dependence of the level of the cavitation noise figure (L_{CNF} [dB, rel. 1 W/m^2 @ 1 Hz m³/Ns]) on the intensity [W/cm^2], which allows to determine the threshold of inertial cavitation in ultrasonic bathes within the frequency range 20-90 kHz.

In this paper, we propose a scaling method based on L_{CNF}–measurements for the effective volume-related ultrasonic power [W/l], besides the frequency the most important parameter of the ultrasonic design. Different borderline cases a) for the sound radiating bottom area and its transducer density (Fig.1) as well as b) for the continuous variation of the filling height h in the tank are considered.

Fig. 1: Examples of sound radiating areas with different transducer densities seen from downside.

As the "active sound radiating area", we define the sum of the surface areas of the front-masses of the transducers, attached to the (bottom) wall of the tank. The active sound radiating area and the distance to the bath surface or the opposite wall then defines a correspondingly calculated sonicated volume of the bath in front of the transducers.

The calculated dependence of the range of ultrasonic action on the extension of the active sound radiating area is exemplary shown for two different cases in Fig. 2 and 3. The sound pressure is calculated as the integral over the velocity potential of the transducer elements as described by Skudrzyk /2/. The blackened areas in both Fig.'s represent those areas, where the threshold of inertial cavitation in degassed water with sonication at 35 kHz is assumed as crossed because the acoustic pressure exceeds 100 kPa there.

Fig. 2 shows this dependence for the two borderline cases of a nearly point-like and a piston-like sound source: the increasing range of inertial cavitation with increasing active sound radiating area becomes clear. Fig.3 shows the decreasing range of inertial cavitation with increasing distances between the transducers at constant active sound radiating area, i.e. for arrays with lower transducer density.

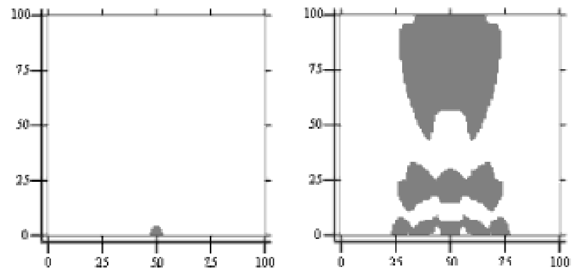

All axis: distance/radius [arb. units]

Fig. 2: Area with a sound pressure above the threshold of 100 kPa for a point source (left) and a rectangular piston (kr=10, right)

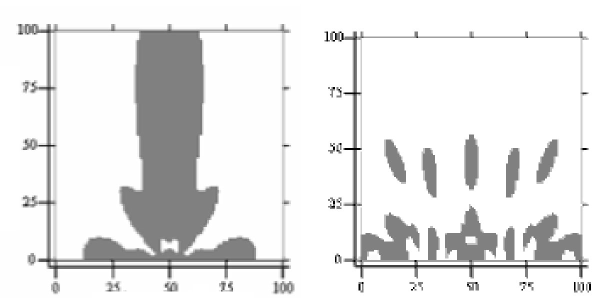

All axis: distance/radius [arb. units]

Fig. 3: Area with a sound pressure above the threshold of 100 kPa for a 3x3 array with small distance (left) and a high distance between the transducers (right)

From Fig.'s 2 and 3 one intuitively expects restrictions for the intended continuous upscaling:

(1) For devices with sound radiating areas at the bottom of the tank, the filling height cannot be smaller than the largest distance between neighbourly assembled bottom transducers.

(2) The range of a sound pressure level sufficient to cross the threshold of inertial cavitation decreases, if the assembled density of the transducer array is lowered and the filling height cannot be larger than this range.

2. Experimental setup and its calculated properties

Fig. 4 shows the experimental setup for the hydrophone measurements used with the 90 litre device Elma S 900 operating at 35 kHz with 16 transducers summing up to 320 cm^2 active sound radiating area on the 500 x 600 mm bottom area and with a maximum filling height of 300 mm.
The distances between the centres of transducers are 140 mm in the long row and 120 mm in the short row.

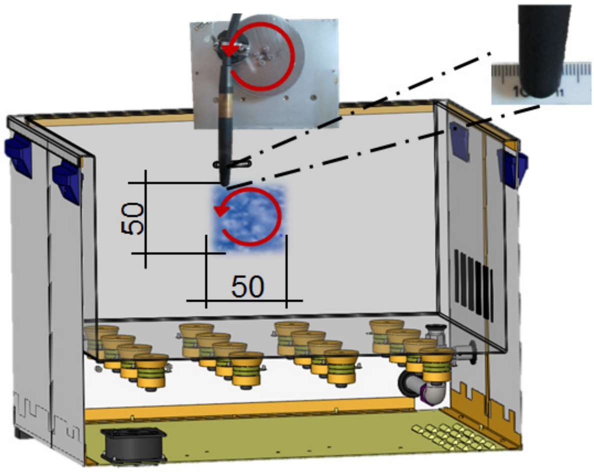

Fig. 4: Experimental setup with moved hydrophone.

Fig. 5 presents the calculated sound pressure level distribution in the S900 along the vertical plane centred between the 2nd an 3rd long row of transducers and taking into account the reflections at the walls and the bath surface for a filling height of 300 mm. This picture shows the need to use a spatially averaging measurement for pressure level and cavitational noise level.

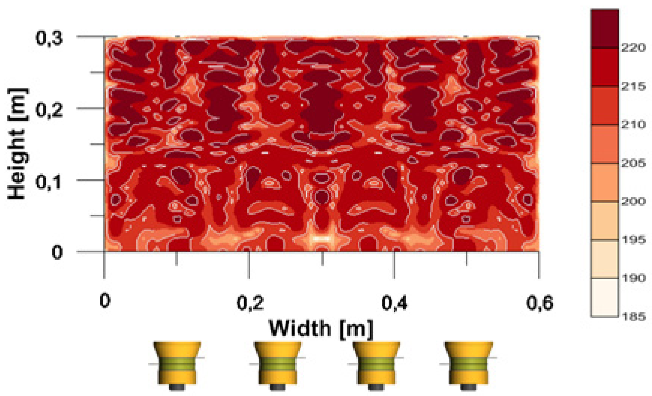

Fig. 5: Sound pressure distribution in dB rel. 1 µPa.

Therefore, the hydrophone is moved up & down and back & forth very slowly below the height of 100 mm to average the sound pressure and the level of cavitation noise L_{CNF}, using the Elma-KaviMeter /1/. This way the variations by

(1) the standing wave pattern of sound pressure (Fig. 5) and

(2) the different sound pressures fields above the transducer and including the pressure maximum along the diagonal line between two transducers of the 1st and 2nd long row of transducers shown in Fig.4

are expressed by the measured values of LCNF also.

3. Measurement results and discussion

The measurements were carried out with ultrasonic devices filled with deionized filtered water of ~40°C and operating at a frequency f_o=35 kHz, modulated with 50 Hz in the double half wave mode (DH). The level of cavitation noise figure L_{CNF} was measured using a calibrated hydrophone Reson TC 4034 as described in /1/.

3.1. Variation of filling height at constant active sound radiating area

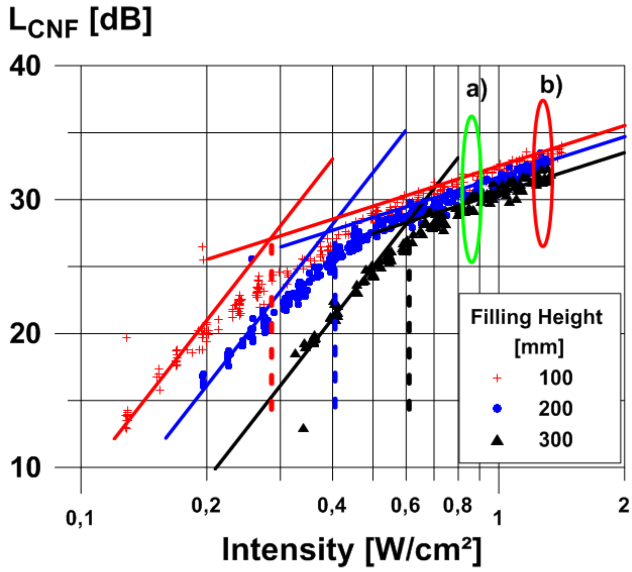

Fig. 6: Measured cavitation noise level L_{CNF} drawn against measured values of the assigned intensities as obtained for the device S900 (see text) at three different filling heights. (Vertical lines mark the break points at thresholds of inertial cavitation. Circles a) and b) mark the region above the thresholds investigated in Fig. 7 in more detail.)

Fig.6 presents for three filling heights the measured cavitation noise level L_{CNF} at measured values of the intensity [W/cm^2], the latter defined as the measured effective electrical power [W] consumed by the 16 transducers, divided by their summed active sound radiating area of 320 cm^2. The crossing of the straight lines marks the break point of the course of the L_{CNF} - intensity dependence.

There are two conclusions derived from Fig. 6:

(1) The intensity necessary to cross the threshold decreases with decreasing filling height.

(2) The L_{CNF}-values at the same intensity increase with decreasing filling height in the region above the break points of the curves.

Following conclusion (2) the dependence of L_{CNF} on the filling height was investigated more thoroughly at two intensities a) and b) and the results are presented in Fig. 7, with filling height scaled logarithmically. If the slope for the measured L_{CNF}-values at 1.5 W/cm^2 is approximated by a regression line, the relation

$$L_{CNF} \sim \log\left(1/\sqrt{filling\ height}\right) \qquad (1)$$

is obtained. The two restrictions, intuitively expected in the introduction, are observed in Fig. 7 as deviations from the line seen for filling heights

- above 220 mm, because there the sound pressure level being no longer sufficient to cross the threshold of inertial cavitation at the lower intensity 0.75 W/cm^2 and

- below 100 mm for both intensities, because there the filling height becomes smaller than the distance between neighboured transducers.

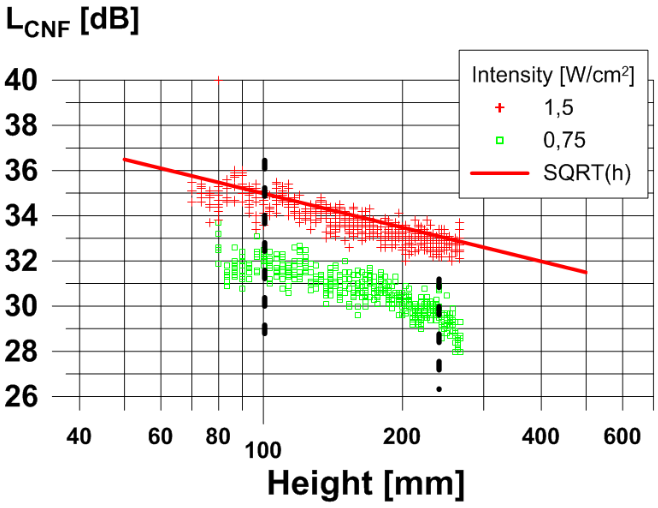

Fig. 7: Measured L_{CNF}-values drawn against filling height as obtained at two intensities for the device S900 (see text).

3.2. Comparison between 2 sound radiating areas of different size at several filling heights and the possibility of normalization to a volume-related power density

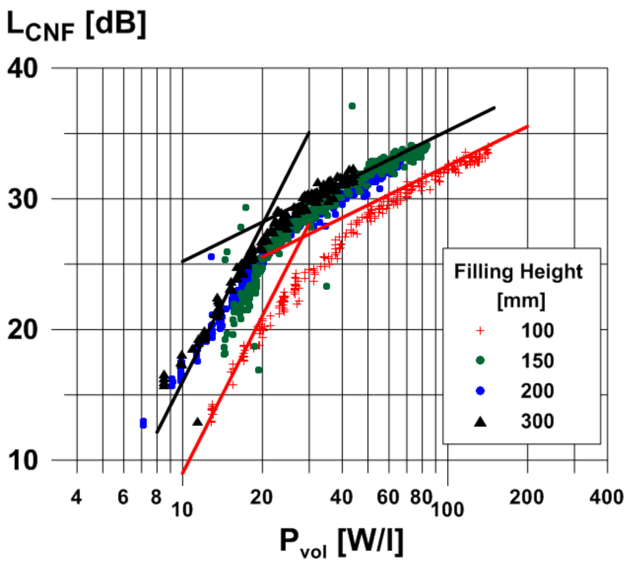

Fig. 8: Measured L_{CNF}-values drawn against the volume-related effective power density (see text), obtained with the device S900 (see text) at four different filling heights.

Fig. 8 presents again the measured cavitation noise level L_{CNF} of Fig. 6 for the S900 device with an active sound radiating area of 320 cm^2. Now the L_{CNF}–values are drawn against the volume-related effective power density [W/l], defined as the measured intensity [W/cm^2], divided by the corresponding filling heights 100, 150, 200 and 300 mm. Again, the crossing of the straight lines marks the break point of the course of the L_{CNF} - intensity dependence, identified as the threshold of inertial cavitation. Now Fig. 8 shows that the break points and curves of L_{CNF} for the filling heights 150, 200 and 300 mm fall together into approximately one common curve with one break point at 27 dB and ~19 W/l if drawn against the volume-related power density [W/l]!

A possible reason why the curve for 100 mm filling height is not expected to coincide with the common curve was given above already.

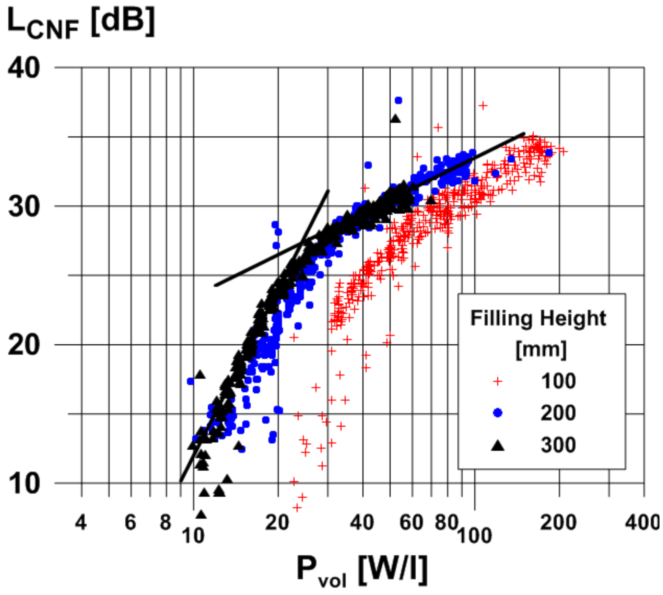

Fig. 9: Measured L_{CNF}-values drawn against the volume-related effective power density (see text), obtained with a device with the half of the S900 bottom area (see text) at three different filling heights.

Fig. 9 shows for three filling heights the measured noise level L_{CNF}-values at measured values of the volume-related effective power density [W/l] for a device with the half of S900 bottom area, i.e. with an active sound radiating area of 160 cm^2 and a correspondingly calculated sonicated volume above 8 transducers. Again the break points and curves of L_{CNF} for the filling heights 200 and 300 mm fall together into nearly one common curve with one break point at 27 dB and ~26 W/l, if drawn against the volume-related power density [W/l]!

Fig. 10 presents the measured noise level L_{CNF} at measured values of the volume-related effective power density [W/l] obtained at same filling height of 200 mm for the S900 (320 cm^2 above 16 transducers) and for the device half of S900 (160 cm^2 above 8 transducers). The curves for the two ultrasonic tanks of different size show the break points at L_{CNF} =27 dB but for the different volume-related power values of 19 and 26 W/l.

- the 2 power densities P_{vol}(V1) = 19 and P_{vol} (V2) = 26 W/l found at the threshold of inertial cavitation and
- the 2 different sonicated volumes V1 and V2=2*V1.

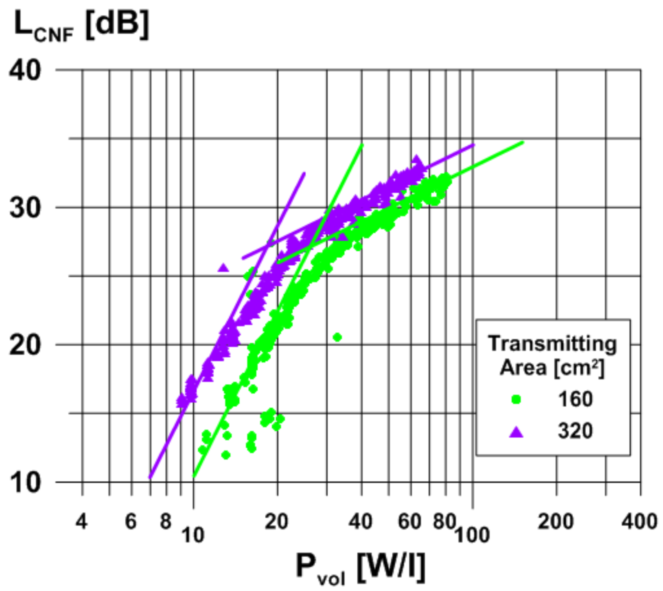

Fig. 10: Measured L_{CNF}-values drawn against the volume-related effective power density (see text) as obtained at filling height 200 mm for the two different sound radiating areas of devices S900 and half of S900 (see text).

So, the volume-related power values at the break points in Fig.'s 8, 9 and 10 suggest a relation of inverse proportionality

$$P_{vol}(V2) / P_{vol}(V1) = \sqrt{V1/V2} \quad (2)$$

similar to Equ. (1) between the limits.

4. Summary and outlook

(1) With decreasing filling height h the level of the cavitation noise figure L_{CNF} changes above the threshold of inertial cavitation approximately according to

$$L_{CNF} \sim log(1/\sqrt{h}).$$

The lower limit for h in this relation is determined by the distance of the transducers, the upper limit by a sound pressure level sufficient to cross the threshold of inertial cavitation.

(2) The level of the cavitation noise figure L_{CNF} at the threshold of inertial cavitation in deionized filtered water of 40 °C at 35 kHz amounts to ~27 dB and does not depend on the filling height or on the active sound radiating area. This value matches the measurements at frequencies of 27 kHz and 45 kHz with a cavitation noise level of 28 dB and 26 dB from /4/.

(3) A relation of inverse proportionality

$$P_{vol}(V) \sim 1/\sqrt{V}$$

between the volume-related power density P_{vol} required at the threshold of inertial cavitation and the calculated sonicated volume V in front of the transducers is suggested be applied for the scaling of the ultrasonic power for tanks of different sizes.

(4) It is intended to check the above-mentioned conclusions for other frequencies of the ultrasound and for further configurations (transducer densities) of active sound radiating areas and filling heights.

5. References

/1/ Sobotta, R.; Jung, Ch.: KaviMeter: Ein Messverfahren zur Bestimmung des Kavitationsrauschens, Fortschritte d. Akustik DAGA2011, 921-922

/2/ Skudrzyk, E.: The Foundations of Acoustics, Springer 1971

/3/ Jung, Ch.; Sobotta, R.: About the Threshold of the Transient Ultrasonic Cavitation in the Cavitational Noise at Different Frequencies, Fortschritte d. Akustik DAGA2009, 1348-1349

/4/ Hertz-Eichenrode, A. et al.: Verhalten des Rauschpegels bei der Kavitationsschwelle für unterschiedliche Frequenzen, Fortschritte d. Akustik DAGA2014, 698-699